A Novel Clay-Biochar Nanocomposite Material for Efficient Removal of Lead from Aqueous Solution

Mohamed Hussein Omar, Njagi Njomo, Amir O. Yusuf, Immaculate Michira, Fanelwa Ajayi & Takalani Mulaudzi

University of Nairobi

ABSTRACT

The research study reports a fresh synthesis of clay-biochar nanocomposite material derived from natural clay and Prosopis Juliflora plant for effective removal of lead metal from aqueous solution. The nanocomposite material was formed by heat pyrolysis of clay and biochar biomass at different temperatures and synthesis was confirmed by characterization with XRF, EDX, FTIR, XRD, and SEM. The characterization revealed successful impregnation of the clay minerals on the surfaces of the biochar material to form the composite material. The efficacy of removal of lead metal by the composite material was ascertained by the batch adsorption method. The three materials of calcined clay, biochar, and composite material all produced a good removal efficacy. Adsorption isotherms of Frendluich and Langmuir to study adsorption were used which showed near to fit adsorption isotherms for lead removal from aqueous solution. The data also showed a pseudo-second-order reaction for the removal of lead metal.

Keywords: a novel, clay-biochar, nanocomposite material, lead, aqueous solution.

Classification: DDC Code: 813.54 LCC Code: PS3553.H15

Language: English

London Journals Press

LJP Copyright ID: 925671
Print ISSN: 2631-8490
Online ISSN: 2631-8504

London Journal of Research in Science: Natural and Formal

Volume 22 | Issue 7 | Compilation 1.0

A Novel Clay-Biochar Nanocomposite Material for Efficient Removal of Lead from Aqueous Solution

Mohamed Hussein Omar[α], Njagi Njomo[σ], Amir O. Yusuf[ρ], Immaculate Michira[Ѡ]
Fanelwa Ajayi[¥] & Takalani Mulaudzi[§]

ABSTRACT

The research study reports a fresh synthesis of clay-biochar nanocomposite material derived from natural clay and Prosopis Juliflora plant for effective removal of lead metal from aqueous solution. The nanocomposite material was formed by heat pyrolysis of clay and biochar biomass at different temperatures and synthesis was confirmed by characterization with XRF, EDX, FTIR, XRD, and SEM. The characterization revealed successful impregnation of the clay minerals on the surfaces of the biochar material to form the composite material. The efficacy of removal of lead metal by the composite material was ascertained by the batch adsorption method. The three materials of calcined clay, biochar, and composite material all produced a good removal efficacy. Adsorption isotherms of Frendluich and Langmuir to study adsorption were used which showed near to fit adsorption isotherms for lead removal from aqueous solution. The data also showed a pseudo-second-order reaction for the removal of lead metal.

Keywords: a novel, clay-biochar, nanocomposite material, lead, aqueous solution.

Author α σ ρ Ѡ: Department of Chemistry, University of Nairobi, P.O. Box 30197, GPO, Nairobi, Kenya.
¥: Department of Chemistry, University of the Western Cape (UWC), Private Bag X17, Bellville 7535-Republic of South Africa.
§: Department of Biotechnology, University of the Western Cape (UWC), Private Bag X17, Bellville 7535-Republic of South Africa.

I. INTRODUCTION

All forms of life on earth depend on water to exist in the ecosystem and it is one of the most essential things for human survival (Obinnaa & Ebere, 2019). Fast population growth, industrialization, and unplanned urbanization are major causes of severe water pollution and surrounding soil. Discharges of toxic industrial and untreated sanitary waste, and runoffs from agricultural land can be major causes of freshwater pollution. Toxic pollutants released into wastewater can be harmful to aquatic organisms, which also make normal water bodies unsuitable for consumption. Studies show that it is a major cause of death and illness around the world killing 1.8 million people in 2015. This makes water pollution a global issue and requires continuous assessment and revision of water resources policies at all levels. The effects of pollution are greater in shallow, confined, or slow-moving streams. Excessive use of fertilizers, herbicides, and pesticides can be life-threatening if washed into the river by rain. Excessive phosphorus in fertilizer leads to serious eutrophication. (Owa, 2014).

Heavy metals are natural elements with a high atomic weight and a density more than five times that of water (Duffus, 2002). Heavy metals are considered trace elements because they are present in various environmental matrices at trace concentrations (ppb range less than 10 ppm). Their bioavailability is affected by physical factors such as temperature, phase association, adsorption, and isolation. Heavy metal pollution in the aquatic environment is a concern for the global environment due to their toxic effects and accumulation through the food chain. Various

London Journal of Research in Science: Natural and Formal

regulatory agencies have set maximum regulatory limits on the emission of toxic heavy metals into water systems. Allowed maximum limits in drinking water for lead metal by different local and international organizations are shown in Table 1 (U.S.EPA, 2009; WASREB, 2006; WHO, 2011; EU, 2018; BIS, 2012).

Table 1: Allowed maximum limits in drinking water for lead ion by different local and international organizations

Organization	Pb (mg/L)
USEPA, EU, WHO, BIS	0.01
KEBS/NEMA/WASREB	0.05

Nevertheless, metal ions are added to the water stream at concentrations much higher than the limits regulated by industrial activities, causing health hazards and environmental pollution. (WHO, 2011). A study of open sewerage in Nairobi, Kenya, showed that sewage and soil samples from open sewerage in the industrial area of Nairobi contained more than the minimum acceptable levels of heavy metals (Kinuthia et al., 2020). Based on WHO, EU and KEBS standards for drinking water, Nairobi Dam water is heavily contaminated with Pb, Cd, Cu and Ni and therefore, it is water is not suitable for human or animal consumption (Ndeda & Manohar, 2014). Some of the health effects of lead include damage to the brain, kidney, sperm damage, increase in blood pressure, abortion and miscarriages, reduced learning abilities in children, nervous system disruptions, disruption in the synthesis of hemoglobin and anemia to name a few (Halim et. al., 2003). Lead bioaccumulates in the bodies of water and soil organisms. The acceptable maximum limit for lead in drinking water is 0.01 mg/L according to USEPA, EU, WHO, and BIS standards.

There are usually several methods used to remove various heavy metal ions. Some of this include: ion exchange, reverse osmosis, ultrafiltration, electrodialysis, precipitation and adsorption process among others. Adsorption is an effective separation process due to its low operating cost and low energy consumption. Moreover, use of natural and green chemistry sources of adsorbents which is assumed low-cost and abundant in nature has gained prominence in the recent research studies of heavy metal remediation. Clay has recently gained prominence as a remediation and clean-up tool for various environmental contaminants including heavy metals (Bhattacharyya et. al, 2006). The usage of natural clay in the remediation of heavy metals has been employed because of its cost- effectiveness (Sdiri et. al, 2012). Due to widespread accessibility and cheaper cost of naturally occurring clay it has become an attractive adsorbent in the remediation of heavy metals from contaminated sources. Biochar is a fine-grain, porous and carbonaceous solid that is produced from waste biomass remains under circumstances with limited oxygen content and low to medium temperatures (450-650°C) by slow pyrolysis (Lehmann & Joseph, 2012). Biochar is a highly porous structure with a large surface area, a high pH, abundant surface functional groups, high cation exchange capacity (CEC), has adsorption ability, contains organic matter, and has high water holding capacity. A composite is a natural or manufactured material composed of two or more materials with dissimilar physical and biochemical properties that are separate and distinct at macroscopic and microscopic scales within the substance (Srinivasan, 2011). Various nanocomposites have been used as adsorbents in heavy metals removal from various matrices in the environment. Kanchana et al., (2012) concluded that the nanocomposite material of chitosan composed of methylcellulose and nanochitosan with kaolin clay in the existence of cross-linking agent performs as a noble adsorbent to eliminate Pb (II) ions from artificial wastewater.

The study presents a novel synthesis procedure for clay-biochar composites material for effective removal of lead ions from aqueous solution. The Biochar was derived from *Prosopis Juliflora* from Northern Kenya.

II. MATERIALS AND METHODS

2.1 Study Area

Natural clay was collected from the Kimathe Valley in the Mukurweini sub-county, Nyeri county (latitude 0° 37' 55.9 ''S, longitude 37° 9' 43.8' 'E) as shown in Figure 1. Random samples were taken from three locations. The collected samples of clay were taken at 500 m intervals in the same area where the clay mines were located. The depth of the samples taken from the surface was 0.45m. The samples were packed in a plastic container then taken to the laboratory for analysis. The sampling of *Prosopis Juliflora* was done purposively on the banks of river Tana, in Garissa county (latitude 0° 27' 50'' S, longitude 39° 38' 12' 'E) as shown in Figure 2. The types of *Prosopis* tree were selected from possibly clean zones as wood biomass supplies for charcoal production. *Prosopis Juliflora* trees were carefully selected by their similar age (which was arrived at by diameter of tree stem), evading defects in trees and possibility of pollution (sampling was done at a distance of approximately 100–150m from any road network and 2000 m from any industrial pollution source).

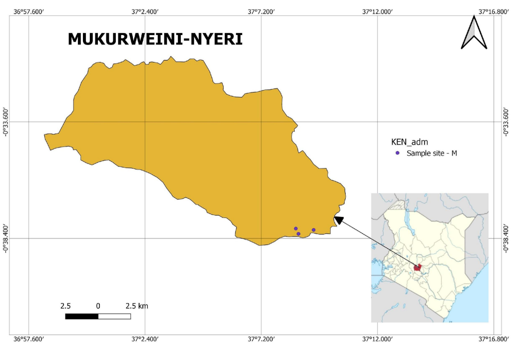

Figure 1: Sampling area in Mukurweini in Nyeri County

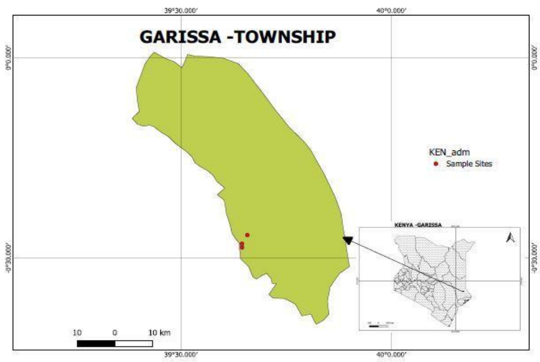

Figure 2: Sampling area in Garissa town in Garissa County

III. MATERIALS AND METHODS

The calcination of the clay was done with a furnace (Daihan FHX, Digital Muffle Furnace, Standard-type, 1200°C, FHX-03/05/12/ 14/27/63) at calcined at 1000 ˚C for a period of one hour. The cut pieces of *Prosopis* were grounded and a fine particle of the ground powder was air-dried for 24 hours to reduce the moisture content. The pyrolysis process was carried out with a furnace (Daihan FHX, Digital Muffle Furnace, Standard- type, 1200 °C, FHX-03/05/ 12/14/27/63). 5g of the feedstock was placed in a ceramic crucible and subjected to heat pyrolysis at different temperatures (200 °C, 400 °C, 500 °C, and 700 °C respectively) for 2 hrs. After the process of pyrolysis was over the furnace was left for some time for the sample to cool to room temperature. The biochars obtained were marked as S-1-1, S-1-2, S-1-3, and S-1-4 for sample S-1, and S-2-1, S-2-2, S-2-3, and S-2-4 for sample S-2 representing 200 °C, 400 °C, 500 °C, and 700 °C respectively as shown in Table 2.

Table 2: Bio-char samples ID at various temperatures

Temperature sample ID	200°C	400°C	500°C	700°C
S-1	S-1-1	S-1-2	S-1-3	S-1-4
S-2	S-2-1	S-2-2	S-2-3	S-2-4

The modified calcined clay obtained and bio-char were fused by heat pyrolysis using a ratio of 1:1 to form a nanocomposite material. Initially, equal amounts of each were used and subsequently varying ratios to achieve an optimum dispersion for impregnation. For the adsorption studies, an equal amount of the clay silicates and biochar (5g each) was used.

IV. CHARACTERIZATION

The calcined clay, biochar and nanocomposite materials were characterized using FTIR (Nicolet 6700 FTIR system, Model: 16F PC), TEM(JEM-2100F), SEM (Model; Quarto S), XRF, EDX, and XRD (Rigaku powder XRD-model ultima IV with conditions of; start angle 5 and stop angle 70; scan speed 5). Elemental analysis of the calcined clay, biochar and nanocomposite materials were done with XRF and EDX. X-ray diffraction of biochar and composite material were performed to determine the phase analysis. Morphology investigation and measurement of size was carried out by Field Emission Scanning Electron Microscopy (FESEM), and Transmission Electron Microscopy (TEM). For FTIR analysis pellets were made using KBr for the analysis.

V. METHOD OF BATCH ADSORPTION

Batch adsorption procedure was used to study the removal efficacy of lead by the calcined clay, bio-char, and nanocomposite materials. 1.000g of lead metal strip/wire (99.99%) purity was dissolved in nitric acid and diluted to 1 liter to give 1000 mg/L. Standard of lead metal (1000 ppm) was diluted in a 1L volumetric flask to achieve a concentration of 1ppm of lead. 25 mL volume of the diluted solution was put in the Erlenmeyer flask and appropriate dosage of the synthesized material were added. pH adjustment was carried out using dilute NaOH or HCl to achieve desired pH. The extent of removal of lead was evaluated by varying different parameters like pH, interaction time, and adsorbent amount (Ahmed et al., 2006). Before the analysis, the samples of adsorption study of different synthesized material for the removal of lead was subjected to filtration using nylon syringe filters with a pore size of 0.22 µm and a diameter of 13 mm from the membrane solution. Inductively Coupled Plasma-Mass Spectrometry (ICP-MS) was used to analyze the concentration of the lead metal ion before and after the adsorption procedure. Batch adsorption procedure was used to study the efficacy of the composite material. Basic quality control and assurance, sample triplicates, sample blanks, and calibration standards protocols were followed. The removal efficiency was calculated based on the reducing concentrations of lead in water of each sample using Equation 1.

$$\text{Percent removal efficiency} = \frac{Ci - Cf}{Ci} \times 100 \qquad (1)$$

Where C_i is the initial concentration of the heavy metal (mg/L) and C_f is the final concentration of the heavy metal in water after the adsorption process (mg/L).The data obtained from experiments were used to test the applicability of various isotherms like Freundlich and Langmuir isotherm models. Pseudo-first-order kinetics and second-order kinetics equations were used to study the involved adsorption kinetics (Sazali et al., 2020).

VI. RESULTS AND DISCUSSION

6.1 Elemental analysis

Elemental analysis of the composition of calcined clay was determined by XRF and EDX. The results showed that the clay was composed mainly of silicates, aluminate and iron among others as shown in Table 3. The elemental analysis of the biochar was done by EDX. Table 4 shows the EDX elemental analysis of the biochar which indicated that it is composed of carbon and oxygen which was consistent with what was reported in the literature of most biochars. This information corresponded well with the EDX analysis as seen in Figure 3. The presence of gold (Au) is attributed to the FESEM instrument used which was coupled with EDX and usually gold is used for sputter coating material in the initial stage of sample preparation.

Table 3: Percentage composition of calcined clay using XRF

Composition	%
Al_2O_3	32.4
SiO_2	55.0
K_2O	1.1
CaO	1.1
Fe	6.1
P_2O_5	0.5

Table 4: Percentage elemental composition of *Prosopis Juliflora* biochar at 500°C

Element	Wt. %
Carbon (C)	62.5
Oxygen (O)	21.1
Potassium (K)	6.0
Calcium (Ca)	5.3
Chloride (Cl)	2.3
Sodium (Na)	1.0

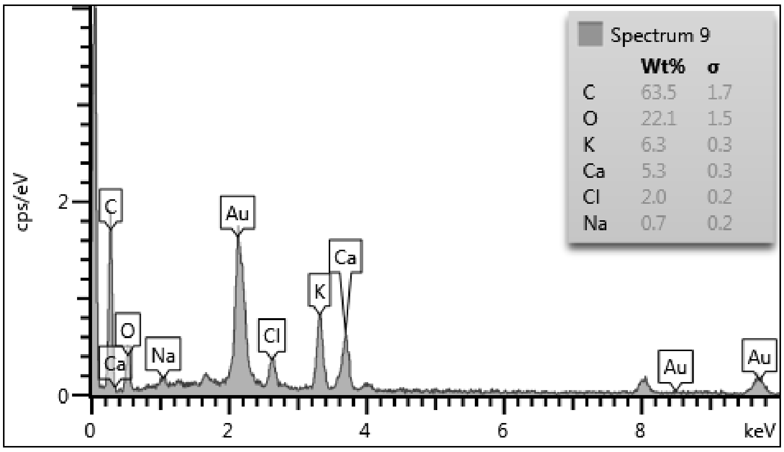

Figure 3: EDX patterns of *Prosopis Juliflora* biochar at 500 °C

The elemental analysis of the nanocomposite material was done with EDX. The results as shown in Figures 4 (A) and (B) showed the elemental composition of the nanocomposite to be high in carbon (C), oxygen (O), silica (Si), aluminium (Al), and iron (Fe). The carbon came from the biochar while the other elements originated from clay material. The average composition was 49.05 % C, 35.85 % O, 5.7 % Si, 5.2 % Al and 2.05 % Fe.

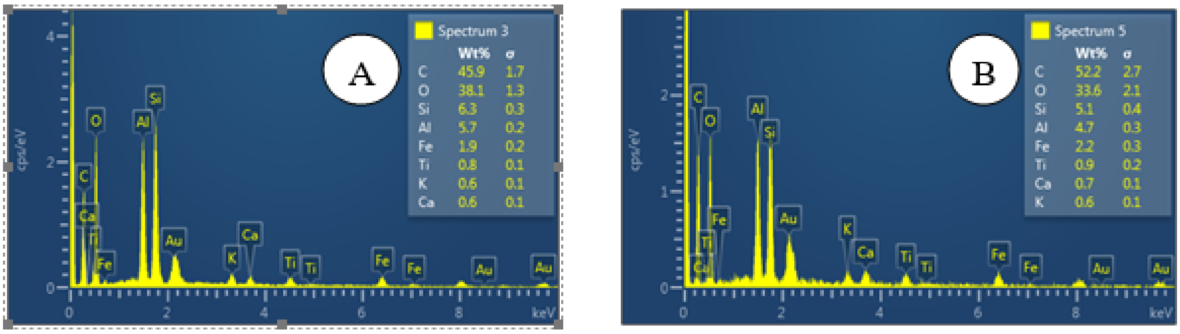

Figure 4: EDX patterns of the nanocomposite material of duplicate (A) and (B)

FTIR

The FTIR spectrum of *Prosopis* Biochar in Figure 5 shows the O-H stretching vibrations of hydrogen-bonded hydroxyl groups at 3500 cm^{-1} bands and the CO_2 absorption peak at 2,350 cm^{-1}. The peak at 1,600 cm^{-1} was attributed to carboxylate (COO^-) and primary amine N-H bending, (Liu et al., 2015), and ~1,405 cm^{-1} was ascribed to aromatic C=C stretch (Zhao et al., 2017). The band around 1,099 cm^{-1} was ascribed to C-O stretching vibrations or the C-N stretch of an aliphatic primary amine (Coates, 2006).

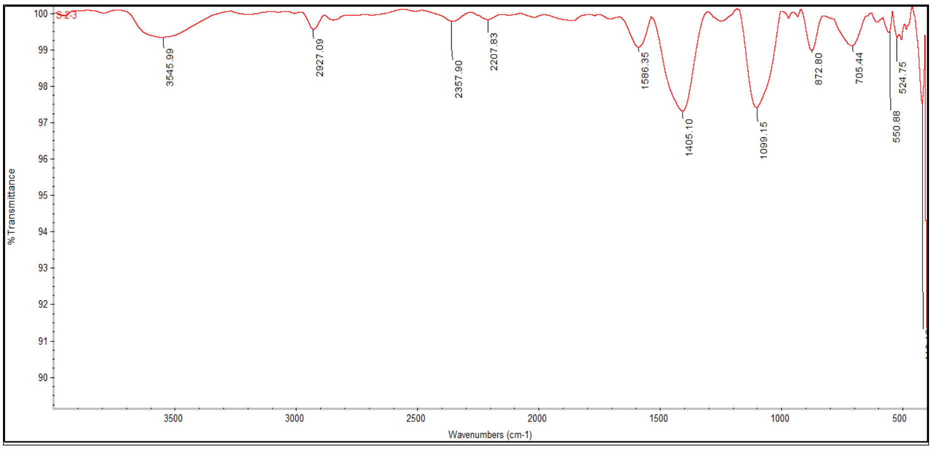

Figure 5: FTIR spectrum of *Prosopis Juliflora* biochar at 500 ° C.

The FTIR spectrum of the nanocomposite material is shown in Figure 6. The spectrum showed a broad weak peak at approximately 3645 cm^{-1} symbolic of O-H stretching as a result of the hydroxyl group and another peak at 2349 cm^{-1} associated with CO_2 absorption. The band at 1,063 cm^{-1} was ascribed to C-O stretching vibrations. This was an indication that the biochar material composition was well contained in the nanocomposite material, therefore successful impregnation of clay silicates on the biochar surface.

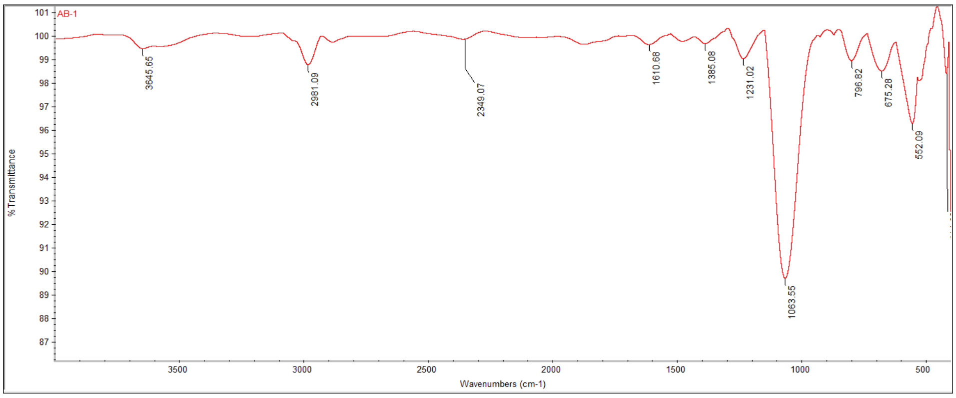

Figure 6: FTIR Spectrum of Nanocomposite Material

XRD

The X-ray Diffraction (XRD) pattern of *Prosopis* biochar is shown in Figure 7. The existence of cellulose or other related organic compounds was shown by the rise in the background level and by a huge hump between 11 and 13° (Fancello et al., 2019). The broad peak at the 2θ values around 23° was related to the crystalline cellulose in the spectrum (Osman et al., 2018). A narrow sharp peak at around 30° was seen and recognized as amorphous carbon (Fu et al., 2016). XRD analysis of clay-biochar nanocomposites showed the existence of mineral crystals. In the spectrum, the three strong peaks at 19.9°, 25°, and 35° were identified as expansible phyllosilicates (Yao et al., 2011) as shown in figure 8. These XRD results agreed well with EDX results that the pyrolysis method had successfully implanted silicates onto the carbon surfaces of the biochar matrix to form a clay-biochar nanocomposite.

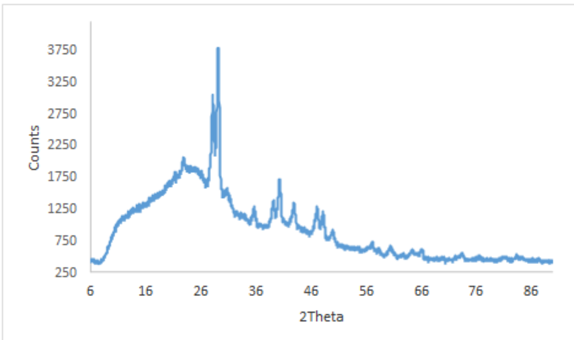

Figure 7: FTIR spectrum of *Prosopis Juliflora* biochar at 500 °C.

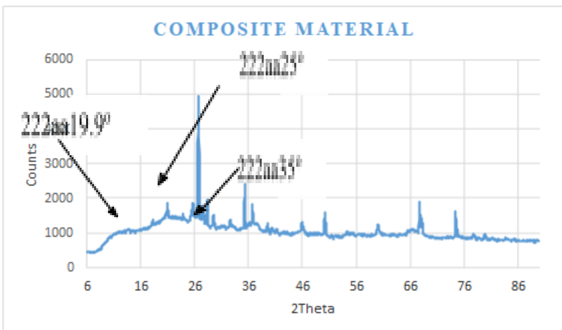

Figure 8: XRD pattern of clay-biochar nanocomposite

SEM and EDX

The images from SEM of biochar revealed two key morphological structures for samples: fibrous structures and pith. As can be seen from Figures 9A, 9B, and 9C the biochar sample was described by rough particles of different sizes with vascular features packed in rolls and had a comparatively flat surface, this had similarly been observed in literature (Zhang et al., 2014; Wang et al., 2015).

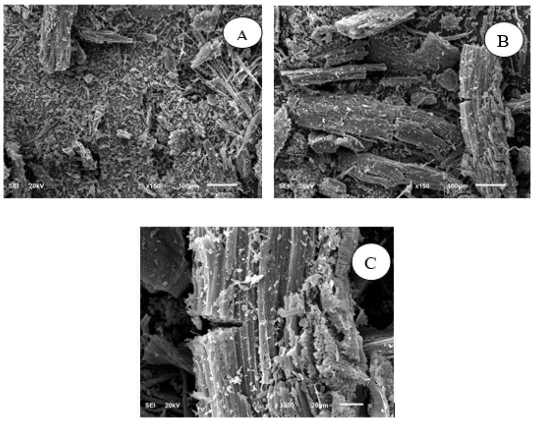

Figure 9: SEM images of the *Prosopis Juliflora* biochar at (A): 100 µm, (B): 100 µm, and (C): 20 µm

The SEM images of the clay biochar composites revealed that the sample surface was mainly covered by thin-film structures as shown in Figure 10 (A). At a higher magnification (X5), the films showed layered surfaces as seen in Figure 10 (B). Structural morphology of calcined clay gave the description as shown in Figure 10 (C) (Wang et al., 2004). The surface covered with clay particles on the biochar was additionally established by the EDX analysis as given in Figure 11. Both the EDX spectrum and the SEM image of the surface revealed high peaks for silicon, aluminum, titanium and iron, all of which are typical of the elemental composition of clay. The SEM images of clay revealed clear morphology of typical clay and the composite displayed successful impregnation of biochar on the surface of the clay minerals as confirmed by EDX analysis.

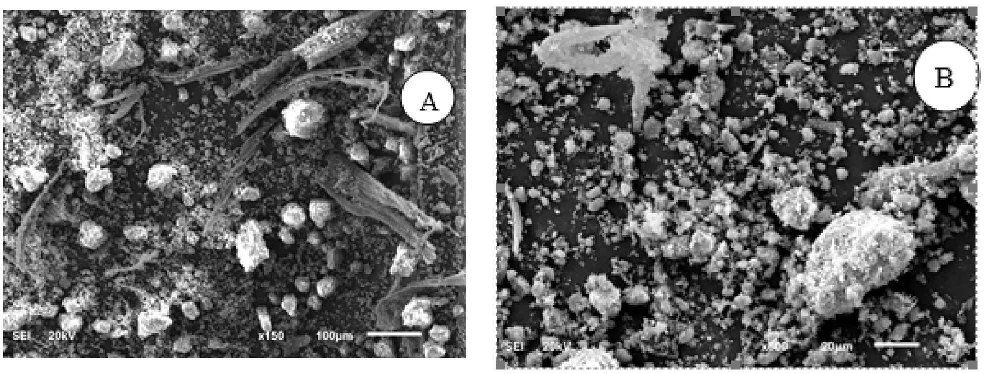

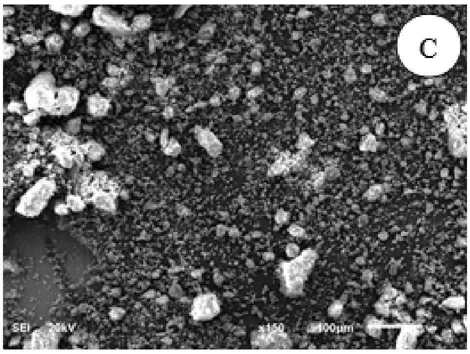

Figure 10 (A-C).: (A): SEM images of nanocomposite at 100 µm; at 20 µm (B) and of calcined clay (C)

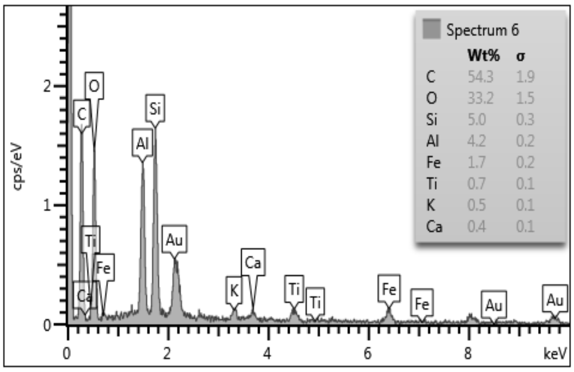

Figure 11: EDX spectrum of the nanocomposite

4.2 Adsorption and efficacy of the composite material

During the batch adsorption analysis, the following parameters were taken into account: pH, contact time, speed of the shaker, and dosage of the material. The data from the adsorption results was not varying for the four heavy metals and the maximum removal was realized after 60 mins of contact time for all the metals which agreed with Rediske (2014). The pH range was between pH 4 – pH 9. The highest removal as seen from the adsorption results at pH 8 was 99.95% removal efficiency for Pb. Therefore, pH 8 was selected as the optimum pH for adsorption of lead ion for the rest of adsorption experiments. For the speed of the shaker, the results from the adsorption for the heavy metals were performed ranging from 50 rpm to 200 rpm using an orbital shaker and maximum efficiency was at 150 rpm.

The removal efficacy of calcined clay for lead ion from aqueous solution was at 99.35 % while biochar was at 99.6 % and nanocomposite material was at 99.8 % (12 (A-C)). Figure 12 (D) showed a summary of the percentage removal of lead ion by calcined clay, biochar and composite material from aqueous solution.

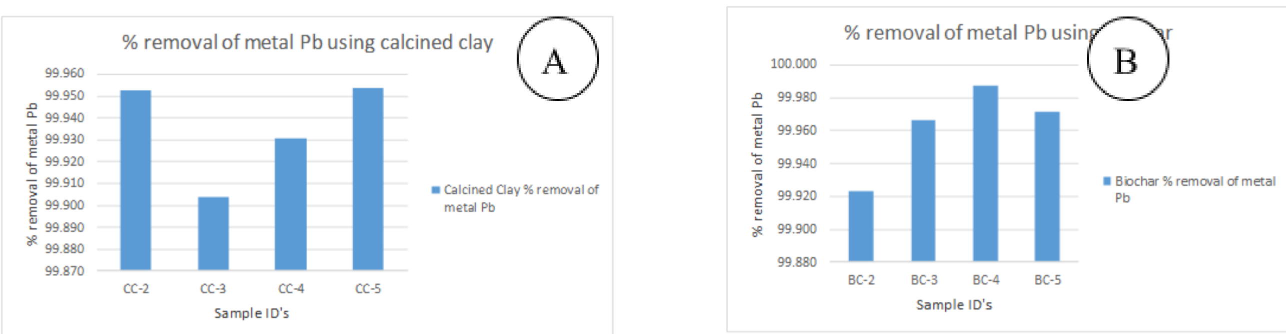

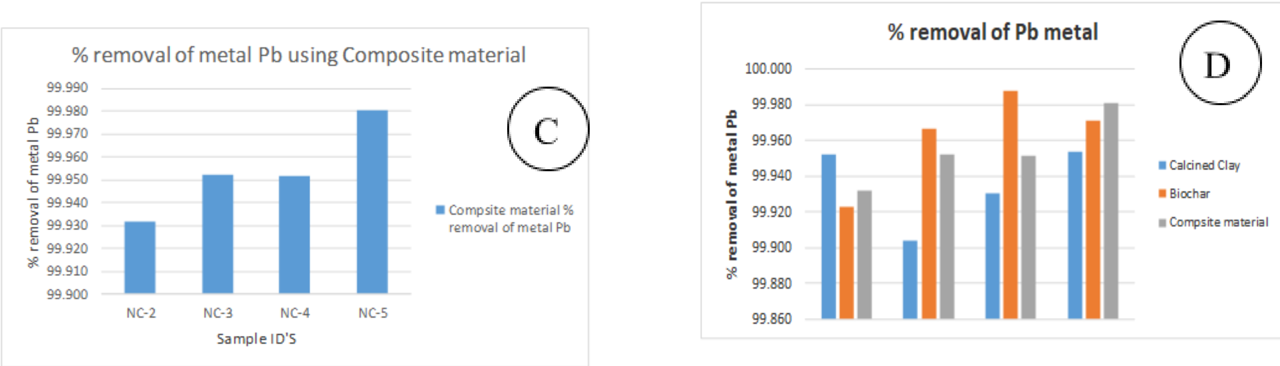

Figure 12 (A-D): removal efficacy of A: calcined clay; B: Biochar; C: composite material and D: summary of % removal of calcined clay, biochar and composite material

4.5 Freundlich and Langmuir isotherms

For Freundlich isotherm adsorption data, calcined clay removal for lead ion gave a poor fit with R^2 of 0.0233, while removal with biochar material had a fit of 0.9978 and composite material had a fit of R^2 of 0.9885 as can be seen in Figures 13(A-C). For Langmuir isotherm adsorption data calcined clay and composite material produced a perfect fit with R^2 of 0.999 while biochar had a fit of R^2 of 0.973 as can be seen in the Figures 14 (A-C).

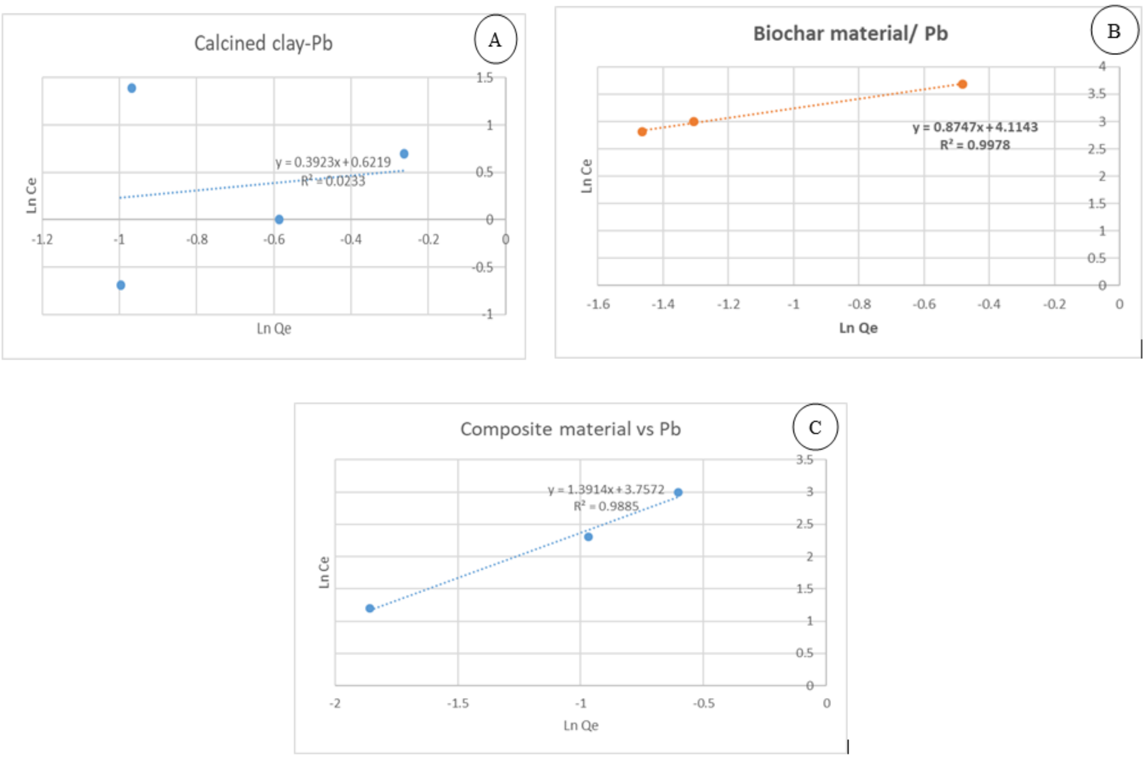

Figures 13(A-C): Freundlich isotherms for A: calcined clay; B: Biochar and C: Composite material for removal of lead metal from aqueous solution.

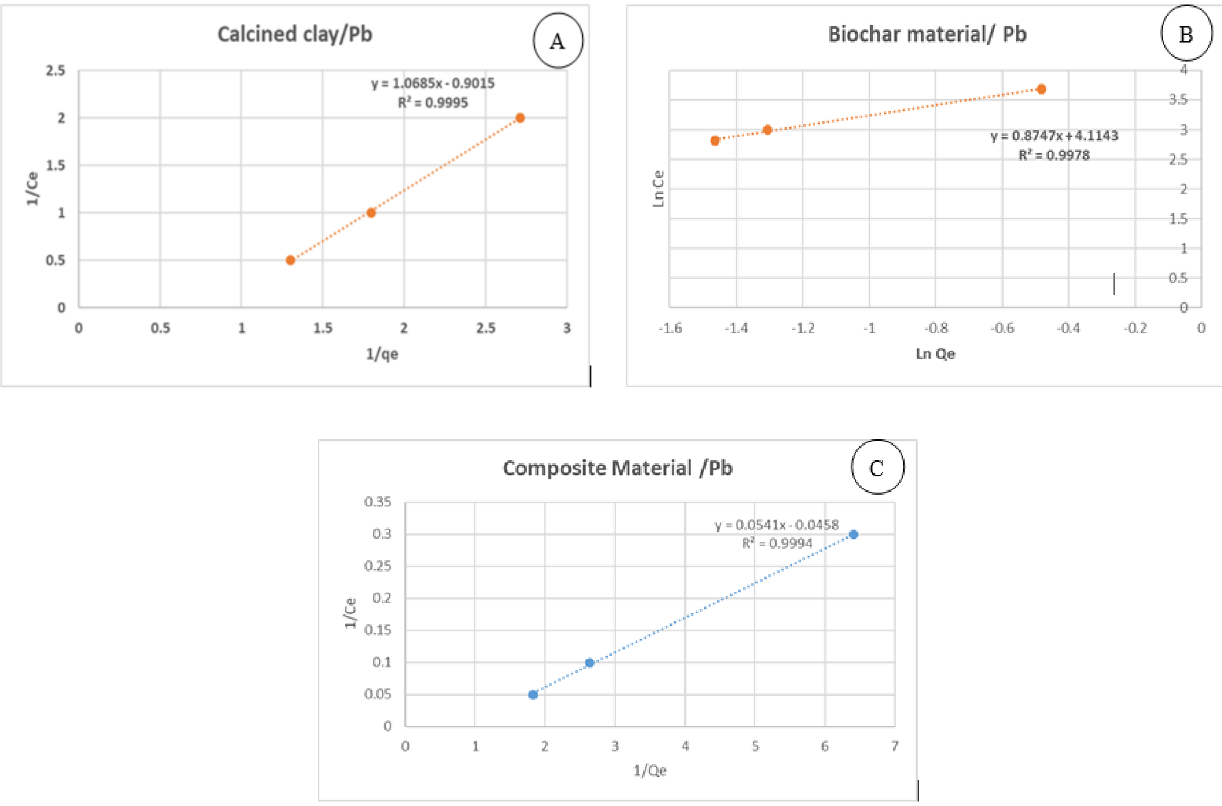

Figures 14(A-C): Langmuir isotherms for A: calcined clay; B: Biochar and C: Composite material for removal of lead metal from aqueous solution

Tables 4 and 5 summarizes the calculated constants for both Freundlich (K_f, n and r^2) and Langmuir (q_m, K_L and r^2) isotherms

Table 5: Freundlich isotherms constants (K_f, n and r^2) for calcined clay, biochar and composite materials for lead metal

Materials	Freundlich Constants		
	K_f	n	r^2
Calcined Clay	0.131	0.824	0.0233
Biochar	14.763	2.359	0.9978
Composite	2.837	1.349	0.9885

Table 6: Langmuir isotherms constants (K_f, n and r^2) for calcined clay, biochar and composite materials for lead metal

Materials	Langmuir Constants		
	K_L	q_m	r^2
Calcined Clay	-36.30	0.151	0.9995
Biochar	19.25	9.116	0.9978
Composite	9.32	2.999	0.9994

The kinetic experiments indicated that the second-order kinetic pseudo-model fits the data better than the first-order pseudo-model. The second-order pseudo model gave straight-line fits while the first-order pseudo model did not. The slope and y-intercept from the linear regression were used to calculate the rate constant for the second-order experiment. The pseudo- second-order kinetics model is explained from a time vs. t/qt linear plot and the resulting parameters are as shown in Figure 13.

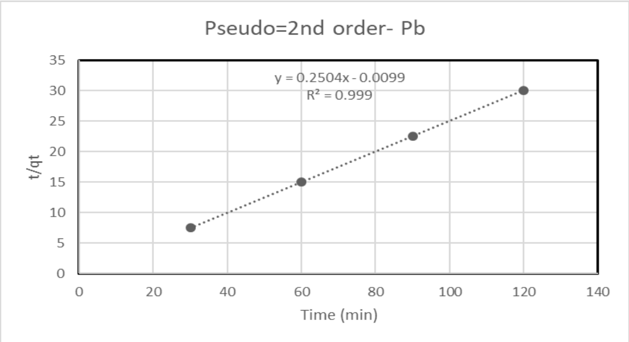

Figure 13: Pseudo second order plot of lead metal

V. CONCLUSION

The study focused on the synthesis of clay-biochar nanocomposite materials derived from clays and *Prosopis Juliflora* feedstock to effectively remove lead ion from aqueous solutions**.** Nanocomposite material was prepared by pyrolysis of clay and biochar biomass at different temperatures, and the synthesized material was characterized by XRF, EDX, FTIR, XRD, and SEM techniques to determine appropriate synthesis. Characterization revealed that the surface of biochar biomaterials was successfully impregnated with clay minerals in the formation of composite materials. The batch adsorption method was used in the study for the removal efficiency of the composite material of the lead ion. All three materials of calcined clay, biochar and nanocomposite produced impressive removal efficiency of lead ions from aqueous solution. Adsorption isotherms of Frendluich and Langmuir were used to study adsorption which confirmed close fit adsorption isotherms for lead elimination from aqueous solution. The results additionally confirmed a pseudo-2nd order reaction for the elimination of lead ion.

Funding support

We wish to appreciate the National Research Fund (NRF-Kenya) for the financial support of the Project.

Conflict of interest

All authors declare no conflict of interest

REFERENCES

1. Bhattacharyya, K. G., & Gupta, S. S. (2006). Pb (II) uptake by kaolinite and montmorillonite in aqueous medium: Influence of acid activation of the clays. Colloids and Surfaces A: Physicochemical and Engineering Aspects, 277 (1-3), 191-200.
2. BIS, I. (2012). Indian Standard Drinking Water Specification (Second Revision). *Bureau of Indian Standards*, *IS 10500*(May), 1–11.http://cgwb.gov.in/Documents/WQ-standards.pdf
3. Coates, J. (2006). Interpretation of Infrared Spectra, A Practical Approach. *Encyclopedia of Analytical Chemistry*, 1–23. https://doi.org/10.1002/9780470027318.a5606
4. EU. (2018). Quality of water intended for human consumption. *Http://Ec.Europa.Eu/Environment/Water/Water-Drink/Review_En.Html*, *0332*(2017), 02/03/ 2018. http://ec.europa.eu/environment/water/water-drink/review_en.html
5. Duffus, J. H. (2002). "heavy metals" - A meaningless term? (IUPAC technical report). *Pure and Applied Chemistry*, *74*(5), 793–807. https://doi.org/10.1351/pac200274050793
6. Halim, M., Conte, P., & Piccolo, A. (2003). Potential availability of heavy metals to phytoextraction from contaminated soils induced by exogenous humic substances. Chemosphere, 52(1), 265-275.
7. Kanchana, V., Gomathi, T., Geetha, V., & Sudha, P. N. (2012). Adsorption analysis of pb(II) by nanocomposites of chitosan with methyl cellulose and clay. *Der Pharmacia Lettre*, *4*(4), 1071–1079.
8. Kinuthia, G. K., Ngure, V., Beti, D., Lugalia, R., Wangila, A., & Kamau, L. (2020). Levels of heavy metals in wastewater and soil samples from open drainage channels in Nairobi,

Kenya: community health implication. *Scientific Reports*, *10*(1), 1–13. https://doi.org/10.1038/s41598-020-65359-5
9. Liu, Y., He, Z., & Uchimiya, M. (2015). Comparison of Biochar Formation from Various Agricultural By-Products Using FTIR Spectroscopy. *Modern Applied Science*, *9* (4), 246–253.https://doi.org/10.5539/mas.v9n4p 246
10. Lehmann, J., & Joseph, S. (2012). Biochar systems. In Biochar for environmental management (pp. 179-200). Routledge.
11. Ndeda, L. A., Manohar, S. 1. (2014). Determination of Heavy Metals in Nairobi Dam Water, (Kenya). *IOSR Journal of Environmental Science, Toxicology and Food Technology (IOSR-JESTFT)*, *8*(5), 68–73.
12. Obinnaa, I. B., & Ebere, E. C. (2019). A Review: Water pollution by heavy metal and organic pollutants: Brief review of sources, effects and progress on remediation with aquatic plants. *Analytical Methods in Environmental Chemistry Journal*, *2*(3), 5–38.https://doi.org/10.24200/amecj. v2.i03. 66.
13. Osman, A. I., Ahmed, A. T., Johnston, C. R., & Rooney, D. W. (2018). Physicochemical characterization of miscanthus and its application in heavy metals removal from wastewaters. *Environmental Progress and Sustainable Energy*, *37* (3), 1058–1067. https:// doi.org /10.1002/ ep.12783
14. Owa, F. W. (2014). Water pollution: sources, effects, control and management. *International Letters of Natural Sciences*, *3*, 1–6. www.ilns.pl
15. Rediske, N. M. (2014). The characterization of the adsorption of cadmium from aqueous solution using natural fibers treated with nanoparticles. Montana Tech of The University of Montana.
16. Sazali, N., Harun, Z., & Sazali, N. (2020). A Review on Batch and Column Adsorption of Various Adsorbent Towards the Removal of Heavy Metal. 2(2), 66–88.
17. Sdiri, A., Higashi, T., Chaabouni, R., & Jamoussi, F. (2012). Competitive removal of heavy metals from aqueous solutions by montmorillonitic and calcareous clays. Water, Air, & Soil Pollution, 223(3), 1191-1204.
18. Srinivasan, R. (2011). Advances in application of natural clay and its composites in removal of biological, organic, and inorganic contaminants from drinking water. *Advances in Materials Science and Engineering*, *2011*. https://doi.org/10.1155/2011/872531
19. U.S. EPA. (2009). National Primary Drinking Water Guidelines. *Epa 816-F-09-004*, *1*, United States Environmental Protection Agency. 7p. https://www.epa.gov/sites/production/files/2016-06/documents/npwdr_complete_table.pdf
20. Wang, H., Gao, B., Wang, S., Fang, J., Xue, Y., & Yang, K. (2015). Removal of Pb (II), Cu (II), and Cd (II) from aqueous solutions by biochar derived from KMnO4 treated hickory wood. Bioresource Technology, 197, 356-362.
21. Wang, Shaofeng, Hu, Y., Zong, R., Tang, Y., Chen, Z., & Fan, W. (2004). Preparation and characterization of flame retardant ABS/montmorillonite nanocomposite. *Applied Clay Science*, *25*(1–2), 49–55. https://doi.org/10.1016/j.clay.2003.08.003
22. WASREB-Kenyan Government-. (2006). Drinking water quality and effluent monitoring guideline. *Water Services Regulatory Board*, 1–36. http://www.waterfund.go.ke/toolkit/Downloads/2. Drinking Water Guidelines. pdf
23. WHO. (2011). Guidelines for Drinking-water Quality. *WHO Library Cataloguing-in-Publication Data*, *4th Edition*, 1–541.
24. Yao, Y., Gao, B., Inyang, M., Zimmerman, A. R., Cao, X., Pullammanappallil, P., & Yang, L. (2011). Biochar derived from anaerobically digested sugar beet tailings: Characterization and phosphate removal potential. *Bioresource Technology*, *102* (10), 6273– 6278. https://doi.org/10.1016/j.biortech.2011.03.006.
25. Zhang, J., Lü, F., Shao, L., & He, P. (2014). The use of biochar-amended composting to improve the humification and degradation of sewage sludge. Bioresource technology, 168, 252-258.
26. Zhao, S. X., Ta, N., & Wang, X. D. (2017). Effect of temperature on the structural and physicoc- hemical properties of biochar with apple tree branches as feedstock material. *Energies*, *10* (9). https://doi.org/10.3390/en10091293.

This page is intentionally left blank